THE ASTROPHYSICAL JOURNAL, 349:57–66, 1990 January 20

BRACKETT LINE SPECTROSCOPY OF BURSTS OF STAR FORMATION IN THE NUCLEI OF GALAXIES

PAUL T. P. HO[1]
Harvard-Smithsonian Center for Astrophysics
SARA C. BECK[1]
Raymond and Beverly Sackler Faculty of Exact Sciences, Department of Physics and Astronomy, Tel Aviv University
AND
JEAN L. TURNER[1]
Department of Astronomy, UCLA
Received 1989 January 3; accepted 1989 July 8

ABSTRACT

We have observed Brα (4.05 μm) and Brγ (2.17 μm) lines with 7".2 spatial and 350 km s^{-1} spectral resolution in seven infrared-bright galaxies. From these measurements, we derive the Lyman continuum flux and the luminosity resulting from young stars. The usual problems of extinction and contamination by nonthermal emission are avoided. The contributions of OB stars to the total luminosities of these galaxies can be estimated and range from insignificant (in NGC 3079) to dominant (NGC 1614 and others). The ratios of Brackett to total infrared luminosity are used to deduce the initial mass function of the star formation activity and thus an age for the star formation process. The activity in the program galaxies can be truly described as bursts because they are surprisingly concentrated in both space and time. Most of the infrared emission appears to be generated in an area on the order of the beam size, that is, in the inner few hundred parsecs of the nuclear region. In several of the galaxies, the star-forming regions may be as young as a few million years. Extremely young starbursts may also be indicated by galaxies where many H II regions appear to be optically thick in the radio continuum. The observed ionization is insufficient to produce the observed 10 μm flux by Lyman heating of dust. Heating by nonionizing photons or nonradiative mechanisms such as shocks may be important.

Subject headings: galaxies: nuclei — infrared: spectra — stars: formation

I. INTRODUCTION

Infrared observations have shown that many galaxies are powerful and predominantly infrared sources that can be as luminous as QSOs (Soifer, Houck, and Neugebauer 1987). Dust reradiation of photons from young O and B stars is a possible mechanism for this emission, but nonstellar components such as shock-heated clouds and active galactic nuclei may also be important. In this paper, we measure the contribution of young stars to the total luminosity and derive the rate and duration of star formation activity in a sample of galaxies that are bright in the infrared. This is the third paper in a series (Beck, Turner, and Ho 1986; Turner, Ho, and Beck 1987; hereafter Papers I and II, respectively) reporting on observations of infrared recombination lines of hydrogen in galaxies. By comparing our results with other data, we hope to constrain the characteristics of nuclear star formation activities.

Infrared spectroscopy has proven invaluable in studies of star formation in both Galactic and extragalactic sources (e.g., Willner *et al.* 1977; Lacy 1980; Papers I and II; see also reviews by Rieke and Lebofsky 1979 and Telesco 1988). The Brα and Brγ transitions of hydrogen are free of contamination by nonthermal processes and are less affected by extinction than are optical recombination lines such as Hα. The only strong sources of Brackett lines on a galactic scale are the dense H II regions of young OB stars, so these lines are reliable diagnostics of recent star formation. Using observations of both Brα and Brγ, one can estimate the extinction, the population of OB stars, and their ages. This type of study has been pursued successfully in extragalactic systems by many groups (e.g., Fischer *et al.* 1983; Rieke, Lebofsky, and Walker 1988; Lester, Harvey, and Carr 1988; Becklin and Wynn-Williams 1987; Depoy, Becklin, and Geballe 1987; Kawara, Nishida, and Phillips 1989). We report here on the spectroscopy of Brα and Brγ emission in seven galaxies, all of which are bright-infrared sources, have companions, and have been suggested as possible starbursts. The observations and analysis are presented in § II. In § III, these seven galaxies are examined, together with similar galaxies observed earlier in this program or by other researchers. By analyzing the possible range of uncertainties in various parameters of our derivations, we show that many of the program galaxies appear to have quite extreme conditions, with OB populations that are likely to be more massive and, in some cases, much younger than seen locally. Conclusions and summary are in § IV.

II. OBSERVATIONS AND CALIBRATION

The Brackett line observations were made on the NASA Infrared Telescope Facility on Mauna Kea on 1985 October 9 and 10. The Cornell Cooled Grating Spectrometer (see Beckwith *et al.* 1983 for description) was used with a 7".2 beam and a velocity resolution of 350 km s^{-1}. For each spectrum, seven to nine wavelengths spaced by half a resolution element were measured, and at least two independent spectra were obtained in each position. Wavelengths were calibrated on laboratory

[1] Visiting Astronomer at the Infrared Telescope Facility, which is operated by the University of Hawaii under contract from the National Aeronautics and Space Administration.

TABLE 1

SAMPLE OF GALAXIES

GALAXY	R.A. (1950)	DECL. (1950)	V_{Hel} (km s^{-1})	D (Mpc)	REFERENCE
Galaxies Observed in Present Work					
NGC 520	$01^h21^m59^s.6$	03°31′53″	2160	30	1, 2
NGC 660A	01 40 21.8	13 23 41	850	11	2
NGC 660B	01 40 21.6	13 23 39	850	11	2
Maffei 2	02 38 08.5	59 23 30	0	4.0	3, 4
NGC 1614	04 31 35.7	−08 40 57	4740	62	1, 5
NGC 3079	09 58 35.0	55 55 16	1130	16	1
NGC 6946	20 33 49.2	59 58 50	80	11	6
NGC 7714	23 33 40.6	01 52 41	2800	40	1, 2
Previous Observations from Literature					
NGC 253	00 45 05.7	−25 33 40	250	3.0	7, 8
NGC 1097	02 44 11.5	−30 29 06	1320	16	1, 9
II Zw 40	05 53 05.0	03 23 06	810	9.2	1, 10
NGC 2903	09 29 20.3	21 43 23	570	6.2	1, 9
M82	09 51 42.6	69 55 01	250	5.8	11, 12
NGC 3690	11 25 41.5	58 50 12	3000	41	1, 13
IC 694	11 25 44.2	58 50 18	3120	41	1, 13
M83	13 34 11.1	−29 36 35	520	3.7	14, 15

REFERENCES.—(1) de Vaucouleurs, de Vaucouleurs, and Corwin 1976; (2) Mirabel 1982; (3) Love 1972; (4) Spinrad *et al.* 1973; (5) Feldman *et al.* 1982; (6) Kennicutt 1979; (7) Aaronson, Mould, and Huchra 1980; (8) Beck and Beckwith 1984; (9) Beck, Beckwith, and Gatley 1984; (10) Wynn-Williams and Becklin 1986; (11) Sandage 1984; (12) Simon, Simon, and Joyce 1979; (13) Beck, Turner, and Ho 1986; (14) de Vaucouleurs 1979; (15) Turner, Ho, and Beck 1987.

lamps and were checked by scanning the Brackett lines in NGC 7027. Fluxes were calibrated with measurements of standard stars with absolute accuracy of ±10% (except for NGC 1614, where the 4 μm uncertainty is about ±20% because the calibration spectra did not extend to the redshift of the galaxy). Spectra have relative accuracies about ±4%. Pointing was established by offsetting from SAO stars every 15 minutes and is accurate to ±1″. Since Brα is usually the stronger line in galaxies, it was sought first. Brγ was observed in those positions where Brα was found.

In Table 1, we list the sample of galaxies that were observed. We have also included from the literature a number of other bright galaxies that have been detected either in Brα or Brγ. Adopted distances are listed with relevant references. In most cases, we used heliocentric velocities corrected for the motion of the local group and a Hubble constant of 75 km s^{-1} Mpc^{-1}. For more nearby galaxies, more accurate estimates of the distances have been made and are adopted. In Table 2, we list the Brackett fluxes and the 2.5 σ upper limits in the case of nondetections. Also included in Table 2 are the ground-based 10 μm

TABLE 2

OBSERVED QUANTITIES

			$S_{10\,\mu m}$		$S_{5\,GHz}$				
GALAXY	$S_{Br\gamma}$ (ergs s^{-1} cm^{-2})	$S_{Br\alpha}$ (ergs s^{-1} cm^{-2})	Flux (Jy)	Aperture	Flux (mJy)	Est. Therm. (mJy)	$S^{IRAS}_{12\,\mu m}$ (Jy)	S^{IRAS}_{FIR} (W m^2)	REFERENCE
NGC 520	≤4(−14)	1.9(−13)	0.46	8″	73	...	0.78	1.6(−12)	1, 2
NGC 660	≤4(−14)	7.3(−14)	0.90	8	94	...	2.02	3.5(−12)	1, 2
Maffei 2	≤4(−14)	1.1(−13)	0.2(1.1)	5.7(18)	70	(20)	3.63	5.9(−12)	3, 4
NGC 1614	7.2(−14)	5.5(−13)	0.84	4.5	37	...	1.39	1.5(−12)	5, 6
NGC 3079	...	≤6(−14)	...	...	87	...	1.25	2.5(−12)	7
NGC 6946	7.9(−14)	2.3(−13)	0.75(1.0)	8.5(12)	34	(4)	2.17	3.3(−12)	4, 8
NGC 7714	4.7(−14)	8.9(−14)	0.25	6	17	...	0.50	5.0(−13)	9, 10
NGC 253	6.2(−13)	4.0(−12)	6.2(6.8)	5.7(16)	1250	(125)	20.52	3.8(−11)	3, 4
NGC 1097	1.1(−13)	...	0.06	5	3	...	1.85	2.6(−12)	11, 12
II Zw 40	3.5(−14)	...	0.20	7.7	16	...	0.46	2.9(−13)	13
NGC 2903	3.5(−14)	1.4(−13)	0.47(0.86)	8.5(2.0)	17	(2)	0.86	2.2(−12)	4, 8
M82	2.4(−12)	1.1(−11)	27	30	3400	(<700)	53.21	5.2(−11)	9, 14, 15, 16
NGC 3690	≤4.6(−14)	4.0(−13)	0.81	5	~40	...	3.73	4.9(−12)	17
IC 694	6.1(−14)	4.8(−13)	0.44	5	~160	...	...	...	17
M83	6.2(−14)	1.9(−12)	0.46(2.6)	8.5(20)	30	(22)	4.72	6.2(−12)	8, 18, 19

REFERENCES.—(1) Condon *et al.* 1982; (2) Condon 1980; (3) Rieke and Lebofsky 1978; (4) Ho *et al.* 1989; (5) Lonsdale, Persson, and Matthews 1984; (6) Ho, Turner, and Beck 1989; (7) Duric *et al.* 1983; (8) Lebofsky and Rieke 1979; (9) Rieke and Low 1972; (10) Weedman *et al.* 1981; (11) Telesco and Gatley 1981; (12) Hummel, van der Hulst, and Dickey 1984; (13) Wynn-Williams and Becklin 1986; (14) Hargrave 1974; (15) Kellermann and Pauliny-Toth 1971; (16) Carlstrom 1988; (17) Gehrz, Sramek, and Weedman 1983; (18) Rieke 1976; (19) Turner, Ho, and Beck 1987.

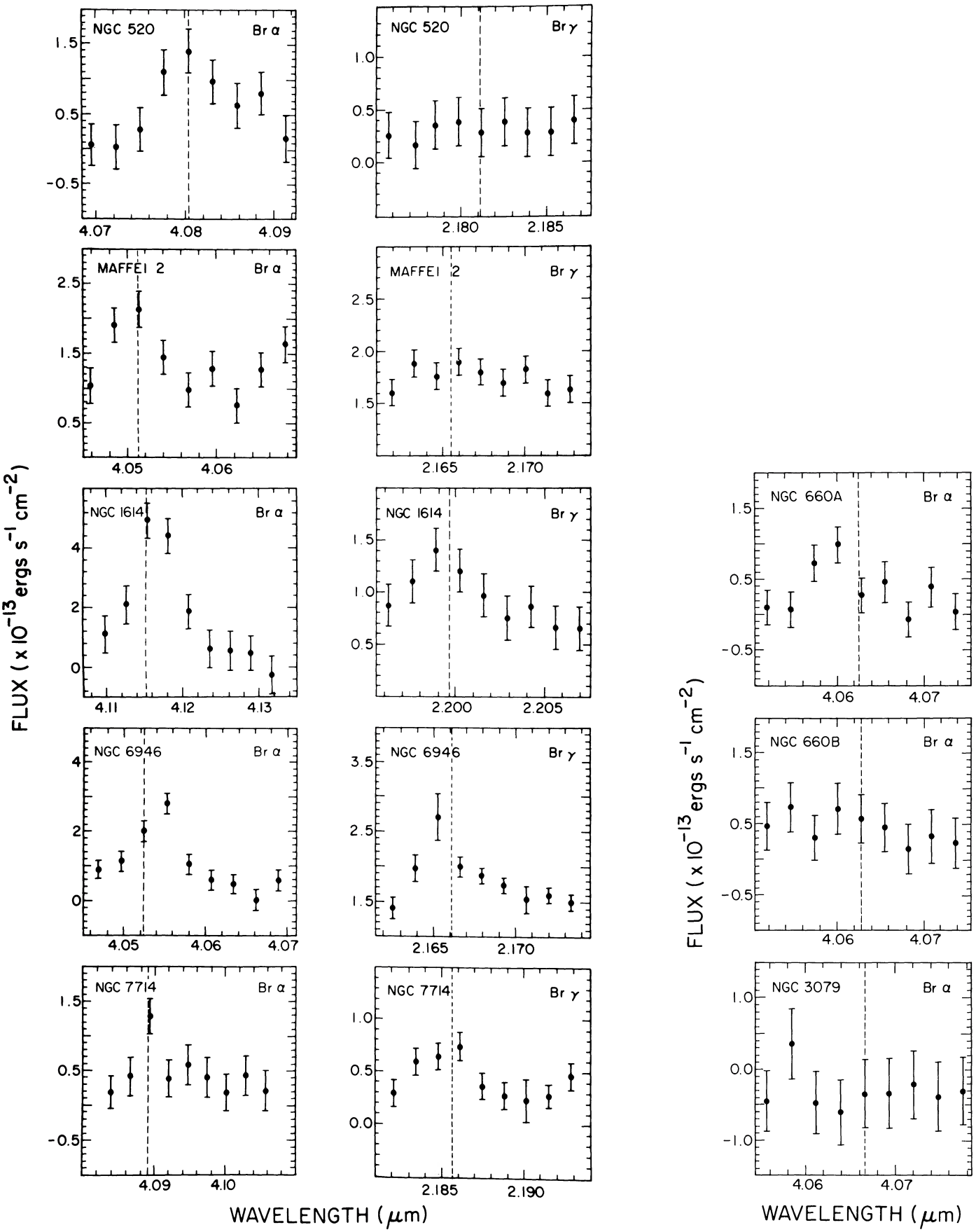

FIG. 1.—Observed spectra. Error bars represent 1 σ uncertainties on a point. Listed fluxes correspond to integration over one resolution element. Flexure of the grating mount may lead to wavelength offsets of up to one-half resolution element. Vertical dashed lines indicate the expected systematic velocities.

TABLE 3

DERIVED QUANTITIES

Galaxy	$A_{4\,\mu m}$ (mag)	$S^{corr}_{Br\alpha}$ (ergs s^{-1} cm^{-2})	$S^{pred}_{10\,\mu m}$ (Jy)	$S^{pred}_{5\,GHz}$ (mJy)	L^{pred}_{OB} $M_u = 30$ ($L_\odot$)	L_{FIR}[a] ($L_\odot$)
NGC 520	>0.23	>2.3(−13)	>0.25	>6.5	>3.7(10)	4.5(10)
NGC 660	>0.00	2.1(−13)[b]	0.23	5.8	4.5(9)	1.3(10)
Maffei 2	>0.03	~1.1(−13)	0.12	3.1	3.2(8)	2.9(9)
NGC 1614	0.46	8.4(−13)	0.92	24	5.8(11)	1.8(11)
NGC 3079	...	≤6(−14)	≤0.07	≤1.7	≤2.7(9)	2.0(10)
NGC 6946	0.00	~2.3(−13)	0.25	6.4	5.0(9)	1.2(10)
NGC 7714	0.00	~8.9(−14)	0.10	2.5	2.5(10)	2.5(10)
NGC 253	0–0.58	6.2(−12)[b]	6.8	170	1.0(10)	1.1(10)
NGC 1097	...	~3.2(−13)[c]	0.35	9.0	1.5(10)	2.1(10)
II Zw 40	...	~1.0(−13)[c]	0.12	3.1	1.7(9)	7.6(8)
NGC 2903	0.15	1.6(−13)[d]	0.18	4.5	1.1(9)	2.6(9)
M82	0–0.28	1.2(−11)[b]	13	340	7.2(10)	5.4(10)
NGC 3690	≥0.52	≥6.5(−13)	≥0.72	≥18	≥2.0(11)	2.6(11)[e]
IC 694	0.48	7.4(−13)	0.81	21	2.2(11)	2.6(11)[e]
M83	0.68–0.99	4.1(−12)	4.5	110	1.0(10)	2.6(9)

[a] L_{FIR} from *IRAS* fluxes.
[b] Over mapped region (data for NGC 660 from J. Fischer 1988, private communication).
[c] Brγ × 2.9, not extinction corrected.
[d] In one 7″ beam.
[e] Includes both NGC 3690 and IC 694.

fluxes and the aperture used, the total radio continuum flux at 5 GHz, and an estimate of the thermal free-free contribution when available, as well as the *IRAS* 12 μm and total far-infrared flux. The observed Brackett spectra are shown in Figures 1*a* and 1*b*.

III. DERIVING GALAXY CHARACTERISTICS FROM BRACKETT LINES

From the Brackett line fluxes, we can estimate the infrared extinction, the Lyman continuum flux, the total luminosity in OB stars, and the expected thermal radio continuum, as well as the expected 10 μm emission if dust heating is due to Lyα photons. The derivations and the associated uncertainties are described in the Appendix. The derived values are given in Table 3. The observed quantities of Table 2 and the derived quantities of Table 3 are compared graphically in Figures 2–5, where the observed Brackett fluxes are plotted against the total infrared luminosity, the radio continuum fluxes, and the 10 μm fluxes.

a) The Total Luminosity

One of the primary issues of interest is the reliability of the Brackett lines as a measure of star formation activity, because extinction may affect even the Brackett lines in large star-forming complexes (Paper II). We assess the role of young stars by comparing the OB star luminosity to the total energy output in each galaxy. For a homogeneous data set, we use the *IRAS* far-infrared fluxes S_{FIR} which are collected in Table 2. From the *IRAS* 100 μm to 60 μm ratio, we can also estimate an effective color temperature for the dust emission. Assuming that the dust radiates at a single temperature, the total luminosity can be calculated from S_{FIR}, as described in the *IRAS* Catalog of Extragalactic Objects. We find this color correction factor to be typically $\lesssim 1.5$. The total infrared luminosity ($L_{FIR} = 4\pi D^2 S_{FIR}$) is listed in Table 3. To examine how much of the total luminosity can be driven by young OB stars, we use the Brackett line strength to find the ionizing flux. For a stellar population with a given mass function, the total luminosity can then be derived from the ionizing luminosity. The relation of the Brackett line flux to the total OB luminosity is derived in detail in the Appendix.

In Figure 2, we compare the observed total luminosity L_{FIR} with the predicted OB luminosity L^{pred}_{OB}. The vertical bars show

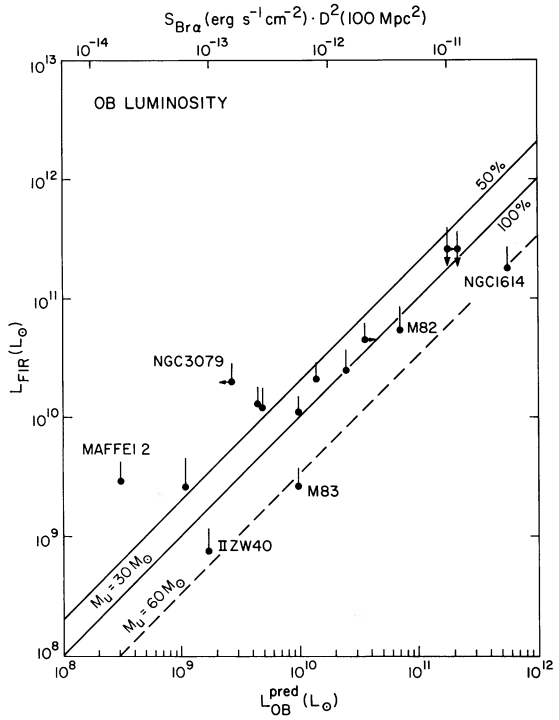

FIG. 2.—The relation of Brα to the far-infrared luminosity. Filled circles show the predicted OB luminosity vs. the *IRAS* far-infrared luminosity. Vertical bars show a color correction to the far-infrared luminosity that assumes that the spectrum is a gray body characterized by a temperature found from the 100/60 μm flux ratio, as prescribed in the *IRAS* Extragalactic Source Catalog. The solid diagonal lines show, for an upper mass limit of 30 $M_\odot$, the expected values of L_{FIR} if 50% or 100% of the luminosity results from OB stars. Dashed line is the 100% expectation for $M_u = 60\,M_\odot$.

the color correction to L_{FIR}. The two diagonal solid lines show the expectations if 50% and 100% of the total luminosity are driven by OB stars whose most massive members have masses $M_u = 30\ M_\odot$. If the upper mass cutoff of the clusters is doubled, the dashed diagonal line shows that the expected OB luminosity would be lower by roughly a factor of 3; i.e., less total luminosity is needed to achieve the same amount of ionization.

We find that for most of the galaxies, L_{OB}^{pred} as derived from the Brackett lines is a major fraction (50%–100%) of the total infrared luminosity. Two galaxies, NGC 3079 and Maffei 2, lie significantly above the expectations. It is almost certain that in these cases a large fraction of the observed infrared luminosity originates from regions outside of the 7″ diameter areas in which we observed the Brackett lines. In NGC 3079, complicated emission along and perpendicular to the galactic disk extends up to 30–60″ from the nucleus (Durie *et al.* 1983). In Maffei 2, the nuclear emission region is extended on the scale of 15″ because it is nearby. The total 10 μm emission is 1.1 Jy in the nuclear region (Ho *et al.* 1989), as compared to 0.2 Jy in the central 5″.7, which suggests that we have not detected all the Brackett emission. In the other two nearby galaxies, NGC 253 and M83, the total infrared luminosities do not exceed the predicted OB luminosities because the Brackett emission in these nuclei has been mapped. The three galaxies II Zw 40, M83, and NGC 1614, whose inferred L_{OB}^{pred} exceed the observed L_{FIR}, appear to require a high value for the upper mass cutoff. A possible explanation is that, in these instances, the burst of star formation is very young where the more massive stars have not yet evolved off the main sequence.

The *IRAS* beam at 100 μm is 3′.0 × 5′.0 (Neugebauer *et al.* 1984), which is large compared to the 7″.2 resolution of the present observations. Remarkably, with the possible exception of NGC 3079, the observed Brackett fluxes can explain the bulk of the total luminosity even without beam size correction. This argues that the far-infrared flux may be due entirely to young OB stars that may not fill the *IRAS* beam uniformly but that are rather concentrated in an area not much larger than 7″.2. In calculating L_{OB}^{pred}, we assumed a Miller-Scalo initial mass function. To obtain agreement with the observed luminosities, we need only tune the age of the burst of star formation. This is not unreasonable, because we are fitting only two parameters, L_{FIR} and the number of ionizing photons N_{uv}. If all the stars are assumed to have formed simultaneously, the starburst can be no older than the main-sequence lifetime of the most massive star. Hence, an upper mass cutoff of $M_u = 60\ M_\odot$ (O5 star) implies an age less than 2×10^6 yr old, while $M_u = 30\ M_\odot$ (O8 star) implies an age less than 7×10^6 yr old. Correcting for the different beam sizes between the Brackett and far-infrared data will move M_u toward earlier spectral types and even younger ages. That galaxies as different in morphology and environment as M82 and M83, or NGC 3690 and NGC 253, have nuclear starbursts characterizable by the same mass function is not too surprising since we are fitting only two parameters. A more sophisticated analysis (e.g., Rieke *et al.* 1980; Rieke *et al.* 1985; Telesco and Gatley 1984), which fits for many parameters including the total stellar mass, the near-infrared flux, and the supernova rate, can constrain further the mass function both on the low-mass and high-mass end. For our purposes of studying the massive star formation rate in the nuclear region, we have not attempted such detailed analysis since extinction effects and peculiar motions would complicate most interpretations.

Because both L_{FIR} and N_{uv} are most sensitive to the massive stars in a cluster, our simple analysis may be reasonable in suggesting that very massive (30–60 $M_\odot$) stars are present in the nuclei of these galaxies. The best way to measure the stellar population in highly obscured regions may be the comparison of the S IV 10.5 μm with the Ne II 12.8 μm emission lines. Phillips, Aitken, and Roche (1984), Beck *et al.* (1978), and Beck, Lacy, and Geballe (1979) searched for one or both of these lines in some of the sample galaxies. They found that Ne II is usually strong and S IV is usually absent or weak. Since S IV requires higher excitation, their absence implies that stars hotter than O9 are not important in the population. However, the S IV line may be affected by a broad silicate absorption feature. Furthermore, upper limits in S IV, especially in regions of high extinction or low luminosity, may not be sensitive enough to rule out the presence of 60 $M_\odot$ stars with a normal initial mass function (IMF), where the Ne II emission and also O III emission (Duffy *et al.* 1987) are used to infer the presence of 30 $M_\odot$ stars.

In summary, by deducing the total ionizing luminosity from the Brackett flux, we can estimate the total infrared luminosity by assuming a mass function for the star formation activity. Compared to the actual observed luminosity, the calculated luminosity from the nuclear region dominates the total integrated luminosity as observed by *IRAS*. This demonstrates that young massive stars may well dominate the luminosity from these galaxies. In a number of cases, if the assumed mass function is applicable, the largest stellar mass needs to be quite high, $\sim 60\ M_\odot$. This argues for an age, perhaps as young as 10^6 yr for the star-forming regions. However, we caution that the mass function that we assume is nonunique. Hence, this scenario should be taken only as a plausible one.

b) *The Radio Continuum Luminosity*

Brackett line fluxes and the thermal radio continuum are both proportional to the ionizing flux. The derivation of the thermal radio flux $S_{5\ GHz}^{pred}$ from $S_{Br\alpha}$ is shown in detail in the Appendix. The calculated values of $S_{5\ GHz}^{pred}$ are compiled in Table 3 and are compared to observed values in Figure 3. The amount of radio emission that is predicted from a given Brackett line flux depends on the electron temperature and (weakly) on the electron density. The solid and dashed diagonal lines reflect the case where 100% of the 5 GHz radio emission is thermal for electron temperatures of 7500 and 5000 K. We have used synthesis radio measurements to obtain angular resolutions comparable to those of the Brackett line observations and to avoid contamination by the nonthermal disk emission.

We find that, in almost all galaxies, the radio emission exceeds the amount predicted by the Brackett fluxes. The implication is that most of the radio emission is nonthermal synchrotron emission, even at arcsecond scales in the nucleus. In the cases where the thermal radio emission can be estimated from spectral index maps, the agreement with the Brackett fluxes is much better. There are three peculiar cases: Maffei 2, NGC 1097, and M83. In Maffei 2, the observed radio flux exceeds the predicted flux by a factor of 3. However, as discussed earlier, the radio emission in Maffei 2 is extended. The observed $S_{5\ GHz}$ is the integrated value (Ho *et al.* 1989), whereas the Brackett flux was for one single 7″.2 beam. If the Brackett emission were mapped, we believe the plotted data point in Figure 3 would be shifted to the right. In NGC 1097, which has somewhat less 5 GHz emission than predicted from the Brackett lines, a ring of H II regions of 20″ in diameter sur-

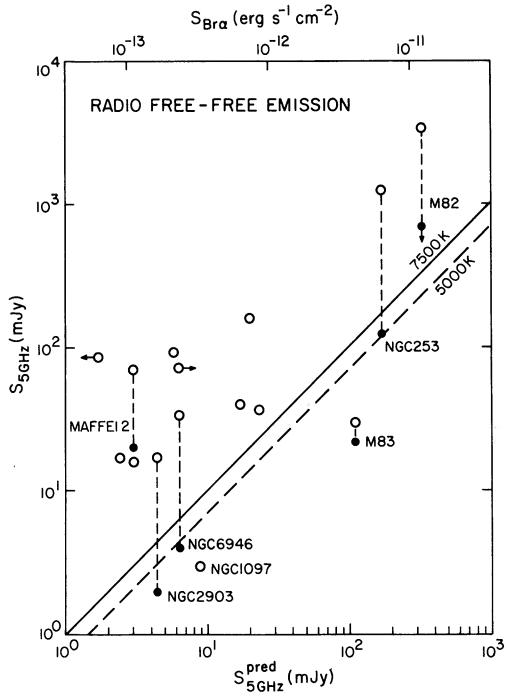

FIG. 3.—The ratio of Brα flux to the observed 5 GHz radio continuum flux. Open circles indicate total 5 GHz fluxes, and filled circles indicate estimates of the thermal free-free radio emission. Solid diagonal line shows the value expected if all radio flux is thermal emission and T_e = 7500 K. Dashed diagonal line shows the case for T_e = 5000 K.

rounds the nucleus (Hummel, van der Hulst, and Dickey 1984). The observed $S_{5\ GHz}$ plotted in Figure 3 does not include this ring of H II regions, but the Brackett observations were probably contaminated. The most peculiar case is M83, where the predicted thermal radio flux is stronger by a factor of 5 than the observed thermal radio flux (see Paper II). This is the only case where the Brackett excess cannot be easily explained by uncertainties in our derivations; e.g., lower values of electron temperatures will not explain the discrepancy. It is possible that other cases of Brackett excesses may be present, especially in more distant galaxies where the spatial resolution is insufficient to resolve such emission complexes. It is also possible that if the thermal radio contributions are found for more of the program galaxies, Brackett excesses with respect to thermal radio fluxes may be more common.

There are several mechanisms that can suppress the thermal radio flux in Galactic sources. In young stellar objects (YSOs) with outflows, the hydrogen lines are often found to be "superluminous" relative to the radio flux (Thompson 1987). However, the luminosity of YSOs is such a small fraction of the luminosity of O stars associated with normal H II regions that we expect the totals on a galactic scale to be dominated by the latter. A second mechanism to explain the Brackett excess is a very low electron temperature in the H II regions. However, the drop in the $S_{5\ GHz}/S_{Br\alpha}$ ratio is only a factor of 2 for a change of T_e from 7500 to 3000 K. Values of T_e below 3000 K are probably unlikely. Another even more speculative possibility is that the Brackett lines arise in the de-excitation of atoms populated in high-n states by nonionizing photons, thereby requiring less ionizing flux. That this is not observed in Galactic sources argues against the likelihood of this model.

Perhaps the simplest explanation for the "Brackett excesses" is that the source is optically thick in the radio but not in the infrared. An ultracompact H II region such as W3(OH), with emission measure $\gtrsim 10^{5-6}$ cm^{-6} pc, will be optically thick at 5 GHz, and such emission measures are reasonable for these galaxies if the emitting gas is moderately clumpy (Paper II). If the excess Brackett emission is due to such objects, more severe limits can be placed on the age of the star formation process. Instead of the main-sequence lifetimes of O stars, we can use the much shorter expansion time scales ($\sim 10^5$ yr) for optically thick compact H II regions. The implication is that star formation in M83 started very recently and with great suddenness. The process must be of relatively short duration or at least episodic in nature because earlier generations of star formation would have left normal H II regions. If the presence of small optically thick H II regions can be confirmed, by radio measurements at short wavelengths or by other means, it may be possible to date the beginning of star formation activity and to search for appropriate triggers in the immediate environs of the nucleus.

In summary, comparison with the radio continuum measurements shows that the Brackett lines are a good measure of the ionizing flux. In the cases where the thermal contribution to the total radio continuum can be assessed, the comparison with the Brackett flux can be used to constrain the age of the star formation activity. We note that, from luminosity arguments, II Zw 40, M83, and NGC 1614 required more massive stars and hence younger ages. Of these galaxies, the thermal radio contribution has been estimated only for M83 and is found to be deficient, again implying a young age. When the thermal radio contributions in II Zw 40 and NGC 1614 can be estimated, we suspect that they will also be found to be deficient compared to the Brackett fluxes.

c) *The* 10 μm *Luminosity*

10 μm photometric observations of galaxies are in wide use as estimators of star formation activity. It is therefore important to check their relation to other star formation diagnostics such as the Brackett lines. Although the *IRAS* 12 μm observations with a 7.5 × 4.5 resolution would provide a homogeneous sample, large-beam measurements may have significant contributions from low-brightness, extended emission such as cirrus. In Figure 4, we checked for this effect by comparing ground-based measurements of nuclear 10 μm luminosity in small beams (Table 2) to the *IRAS* 12 μm flux. For the nearby galaxies M83 and Maffei 2, we use the integrated ground-based 10 μm fluxes. We find that the nuclear and total luminosities are well correlated, with the nuclear emission accounting for typically 50% of the total midinfrared flux. The one exception is NGC 1097, where the 10 μm emission from the ring of H II regions is not included in the ground-based measurement but dominates the *IRAS* flux measurement. Figure 4 shows that, like the infrared luminosity and radio continuum emission, 10 μm in the nuclear region dominates the total 10 μm emission in these galaxies.

If the 10 μm flux is a result of dust heated by Lyα photons from OB stars, then the 10 μm luminosity can be predicted from the Brackett line flux. This is derived in the Appendix. In Figure 5, we compare observed $S_{10\ \mu m}$ with the predicted $S^{pred}_{10\ \mu m}$ from Brackett fluxes. They solid diagonal line shows the expected 10 μm emission when the grain emissivity goes as λ^{-2} with a grain temperature of 200 K. We show in the Appendix that this is an *upper* limit to the expected 10 μm flux. More likely cases are grain emissivities proportional to λ^{-1} or λ^0.

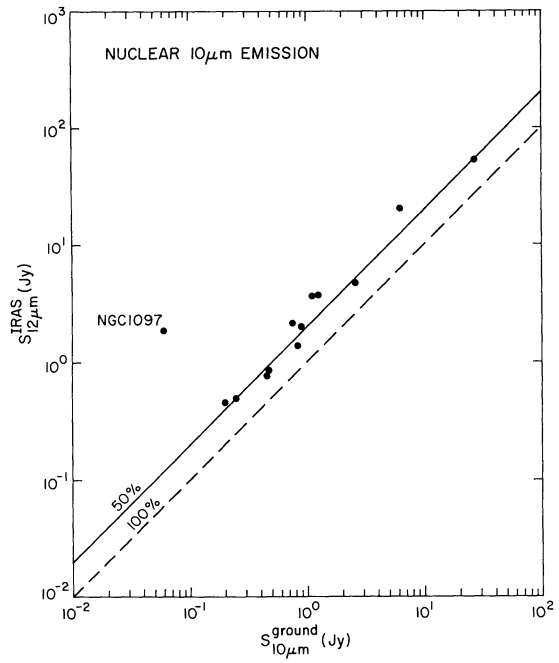

FIG. 4.—*IRAS* 12 μm flux vs. the 10 μm ground-based observations. For M83 and Maffei 2, we have used integrated ground-based fluxes. It is clear that the nuclear emission dominates the total emission seen with *IRAS*.

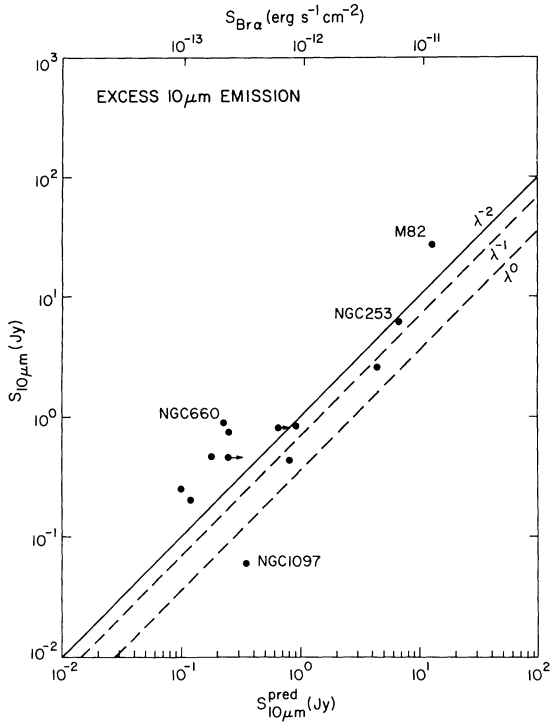

FIG. 5.—Brα fluxes vs. 10 μm fluxes. Diagonal lines show the expectations for different grain emissivities. λ^{-1} and λ^{0} are probably more reasonable estimates. In any case, the 10 μm emission is, in general, in excess of the expected values that were derived assuming Lyα heating. The anomalous point for NGC 1097 is due to the fact that ground-based 10 μm observations do not include the prominent ring of H II regions that are at 10″ from the nucleus and that probably contaminate the Brackett observations.

These are shown as dashed diagonal lines in Figure 5. Hence, although there is a general correlation between the 10 μm intensity and the Brackett line intensity, the important point here is that there is a striking excess of 10 μm emission over the expected values even for extreme grain properties (e.g., λ^{-2} emissivity). Phenomena that could increase the 10 μm flux while leaving the total luminosity in agreement with the Brackett flux may include late-type stars, stars that do not produce detectable ionization but emit strongly at wavelengths just long of the Lyman limit, very small grains, or dust heating by collisions with fast electrons in shocks.

It should be emphasized that the excess 10 μm emission above the value expected from Lyα heating seems unavoidable. There are no reasonable adjustments that can be made to the dust or electron properties in order to boost the dust heating. The heating source for the excess 10 μm emission must be nonionizing in nature. We can probably reject late-type stars from surface brightness arguments. The observed 10 μm brightness in these nuclei is typically $\sim 10^3$ MJy sr^{-1}, which is $\sim 10^2$ times the value of less than 2 MJy sr^{-1} observed in M31, where late-type stars are thought to dominate. We can probably also reject heating by low-mass stars whose luminosities emerge predominantly longward of the Lyman limit. These lower mass stars can produce substantial amounts of luminosity. However, in order for 10 μm emission to be strong, dust temperatures have to reach ~ 200 K, which will be difficult to achieve for lower mass stars.

We favor stochastic collisional excitation of small grains in a hot gas. The presence of very small grains was first suggested by Sellgren (1984), and the associated midinfrared spectra have been suggested to be due to polyatomic aromatic hydrocarbons (Léger and Puget 1984). In a number of nearby galactic nuclei, the 10 μm emission is found to be well correlated spatially with nonthermal radio continuum emission. It is possible that small grains produced and replenished by dust destruction mechanisms associated with supernovae remnants are stochastically heated by collisions with energetic electrons (Ho *et al.* 1989). The presence of a large population of small grains is supported by midinfrared spectra of star-forming galaxies, which show strong, broad-line (UIR) features (Roche and Aitken 1985). The electrons that are responsible for dust heating are in the keV range, while the higher energy relativistic electrons are responsible for the radio synchrotron emission. In this scenario, the 10 μm emission is not a reliable quantitative measure of the star formation rate, unlike the Brackett lines, and may instead be related to the supernova remnants associated with these massive young stars.

In summary, the observed Brackett fluxes are insufficient to explain the observed 10 μm emission fluxes. We suggest that some other dust heating mechanisms, other than Lyα heating, must be present to increase the 10 μm emission. Heating of small grains by energetic electrons may be a viable scheme.

IV. CONCLUSIONS

The Brackett line measurements reported on in this series of papers have proven to be extremely useful in locating star formation sources and in probing the nature and behavior of the OB stars. We have found active star formation to be present in galaxies that vary from each other by factors of several hundred in total luminosity and that range in morphology from apparently normal spiral to so highly disturbed as to fit no Hubble type. Neither morphology nor history proved to be clear predictors of the OB star population. The strong-

est star-formation sites include a tidally interacting pair (NGC 3690 + IC 694), a double-tailed object that may be post-collision (NGC 1614), and a normal spiral galaxy with no convincing evidence of interaction at all (M83).

By comparing the Brackett line measurements to continuum quantities related to them, we estimated characteristics of the stellar population. Our conclusions are independent of distance estimates. Uncertainties in our derivations are well understood. Our results are suggestive of extreme conditions of star formation.

1. There are enough OB stars in the 7".2 beam of these observations to produce most of the far-infrared emission observed with much larger beams. Star formation and the total luminosity in this sample of galaxies therefore appear to be dominated by activities within the inner few hundred parsecs of the nuclear regions.

2. In many of the galaxies, very massive stars appear to be the major components of the luminosity, implying that the starburst is not more than a few million years old.

3. Galaxies whose total luminosities are the same may require different upper mass cutoffs in their stellar population. This may be a function of the age of the burst of star formation. This conclusion, however, is based on the assumption that the OB stars have a normal initial mass function.

4. The thermal radio flux appears to be suppressed in some galaxies. We believe this is probably a result of the presence of optically thick H II regions. If true, this implies that star formation in those galaxies is extremely recent, perhaps as young as 10^5 yr.

5. The 10 μm emission exceeds that predicted from Brackett fluxes and must have dust heating sources other than Lyα photons from OB stars.

We thank Steve Beckwith and Mike Skrutskie for the loan of the equipment and help with the observations, the staff of the IRTF for assistance, and Rodger Thompson and Ed Salpeter for helpful discussions. The observations were supported in part by Northeastern University RSDF grant 7413. P. T. P. H. is partially supported by NSF grants AST85-09907 and AST87-20759.

APPENDIX

DERIVING GALAXY CHARACTERISTICS FROM BRACKETT FLUXES

There are a number of useful quantities that can be derived from the Brackett line measurements. Although such derivations are not new, we collect them here and examine in detail the sources of uncertainties and the explicit dependencies on various parameters. Interesting quantities are then summarized in tables.

I. EXTINCTION

The extinction at near-infrared wavelengths, although small, is not always negligible. Since the Brackett lines will have a characteristic intrinsic flux ratio of Brα/Brγ, the measured flux ratio can be compared to the predicted to give the differential reddening between 2.17 and 4.05 μm, $A_\gamma - A_\alpha = 2.5 \log_{10}(\mathrm{Br}\alpha/\mathrm{Br}\gamma)_{\mathrm{obs}} - 2.5 \log_{10}(\mathrm{Br}\alpha/\mathrm{Br}\gamma)_{\mathrm{intrinsic}}$. The intrinsic ratio can be found from the recombination theory calculations of Brocklehurst (1971), Giles (1977), and Hummer and Storey (1987) and is shown in Table 4 for a range of T_e and n_e. We have adopted $(\mathrm{Br}\alpha/\mathrm{Br}\gamma)_{\mathrm{intrinsic}} = 2.93$, corresponding to $n_e = 10^4$ cm^{-3}, $T_e = 7500$ K. The total extinction at 4.05 μm is then found by assuming that the extinction follows a $\lambda^{-\beta}$ law, $A_\alpha = (A_\gamma - A_\alpha)[(\lambda_\gamma/\lambda_\alpha)^{-\beta} - 1]^{-1}$. For our calculations, we have adopted the emissivity index $\beta = 1.9$ over the wavelengths of concern (Draine and Lee 1984). Because the extinction corrections at these wavelengths are low, the corrected fluxes will not change by more than 10% for changes in T_e and n_e by factors of 2 and 10^2, and changes in β by ± 0.2. The extinctions found are listed in Table 2.

II. RADIO FREE-FREE EMISSION

Lyman continuum fluxes can be derived from the extinction-corrected Brackett fluxes. The number of ionizing photons is obtained from the Brackett line luminosity and recombination coefficients:

$$N_{uv} = \frac{L(n \to 4)\alpha^{(2)}}{h\nu_{n\to 4}\,\alpha_{n\to 4}} = \frac{L(n \to 4)\alpha^{(2)}}{h\nu_{4\to 2}\,\alpha_{4\to 2}} \left[\frac{j(4 \to 2)}{j(n \to 4)}\right],$$

where L is the line luminosity, α's are effective recombination coefficients, $\alpha^{(2)}$ is the sum of recombinations excluding the $n = 1$ level, and j's are the relative intensities of the transitions. These quantities are functions of T_e and n_e and have been computed by Brocklehurst (1971), Giles (1977), and Hummer and Storey (1987). Hence, it is possible to derive N_{uv} as a function of the Brα luminosity $L(5 \to 4)$, or the number of Brα photons. The ratio of ionizing to Brackett photons is shown in Table 5 for a range of T_e

TABLE 4

INTRINSIC VALUE OF Brα/Brγ

T_e (K)	n_e 10^4 cm^{-3}	n_e 10^6 cm^{-3}
3.0×10^3.....	3.27	2.99
5.0×10^3.....	3.06	2.89
1.0×10^4.....	2.82	2.74
2.0×10^4.....	2.64	2.61

TABLE 5

RATIO OF IONIZING PHOTONS ABSORBED TO Brα PHOTONS EMITTED

T_e (K)	n_e 10^4 cm^{-3}	n_e 10^6 cm^{-3}
3.0×10^3.....	8.5	9.9
5.0×10^3.....	10.1	11.4
1.0×10^4.....	13.2	14.1
2.0×10^4.....	17.2	17.9

TABLE 6

RADIO QUANTITIES

T_e (K)	$N_{uv}/L(\mathrm{Br}\alpha)$ (ergs^{-1})	a	$\alpha^{(2)}$ (s^{-1})	$S_{5\,\mathrm{GHz}}/S_{\mathrm{Br}\alpha}$ (mJy/10^{-12} ergs cm^{-2} s^{-1})
3.0×10^3.....	1.73×10^{13}	0.957	6.78×10^{-13}	13.0
5.0×10^3.....	2.06×10^{13}	0.978	4.55×10^{-13}	19.8
7.5×10^3.....	2.41×10^{13}	0.989	3.29×10^{-13}	28.1
1.0×10^4.....	2.69×10^{13}	0.994	2.59×10^{-13}	36.1

and n_e. We find $N_{uv} = 11.8\, N_{\mathrm{Br}\alpha}$ for $n_e = 10^4$ cm^{-3} and $T_e = 7500$ K. For $3000 \lesssim T_e \lesssim 20{,}000$ and $10^2 \lesssim n_e \lesssim 10^4$, this ratio changes by less than $\sim 50\%$.

Lyman continuum fluxes can also be derived from the thermal (free-free) radio fluxes. For example, the radio flux can be derived from the electron density

$$S_\nu = 8.20 \times 10^{-13}\ \mathrm{mJy}\ a\left(\frac{T_e}{\mathrm{K}}\right)^{-0.35}\left(\frac{\nu}{\mathrm{GHz}}\right)^{-0.1}\frac{1}{D^2}\int n_e^2\, dV\ ,$$

where a is a correction factor of order unity (Mezger and Henderson 1967), D is the distance, and dV is the volume element. From recombination theory, and the Brα fluxes, we can derive n_e^2 and therefore deduce the thermal radio flux at 5 GHz

$$S^{\mathrm{pred}}_{5\,\mathrm{GHz}} = 28.1\ \mathrm{mJy}\left(\frac{T_e}{7500\ \mathrm{K}}\right)^{-0.35}\left(\frac{a}{0.9888}\right)\left(\frac{\nu}{5\ \mathrm{GHz}}\right)^{-0.1}\left(\frac{\alpha^{(2)}}{3.29 \times 10^{-13}}\right)^{-1}\left(\frac{N_{uv}/N_{\mathrm{Br}\alpha}}{11.8}\right)\left(\frac{S_{\mathrm{Br}\alpha}}{10^{-12}\ \mathrm{ergs\ s^{-1}\ cm^{-2}}}\right).$$

This relation is independent of geometry and distance. Since a, $\alpha^{(2)}$, and $N_{uv}/N_{\mathrm{Br}\alpha}$ all depend on T_e, we list in Table 6 the expected values for $S^{\mathrm{pred}}_{5\,\mathrm{GHz}}$ for $n_e = 10^4$ cm^{-3} and a range of T_e. The uncertainty in $S^{\mathrm{pred}}_{5\,\mathrm{GHz}}$ resulting from T_e is $\sim 30\%$. The uncertainty in $S^{\mathrm{pred}}_{5\,\mathrm{GHz}}$ resulting from n_e is through the ratio $N_{uv}/N_{\mathrm{Br}\alpha}$ and is $\sim 10\%$ for a factor of 10^2 in n_e.

III. 10 μm EMISSION

If dust heating results entirely from Lyα heating, the total infrared flux can be estimated from the number of Lyman continuum photons, which in turn can be derived from the observed Brα fluxes (see Genzel *et al.* 1982; Ho *et al.* 1989). We can write

$$S_{\mathrm{IR}} = 4.04 \times 10^{-10}\ \mathrm{ergs^{-1}\ cm^{-2}}\left(\frac{N_{uv}/N_{\mathrm{Br}\alpha}}{11.8}\right)\left(\frac{S_{\mathrm{Br}\alpha}}{10^{-12}\ \mathrm{ergs\ s^{-1}\ cm^{-2}}}\right).$$

This relation assumes one Lyα photon for each Lyman continuum photon. To estimate the 10 μm flux, we assume that the dust grains will radiate as a blackbody with a power-law dust emissivity $Q_\lambda \propto \lambda^{-\beta}$. In Table 7, we give the expected values for $S_{10\,\mu\mathrm{m}}/S_{\mathrm{IR}}$ in $\mu\mathrm{m}^{-1}$ units, as a function of β and dust temperatures. We adopt the highest value, obtained for an emissivity law λ^{-2} and a grain temperature of 200 K. The expected 10 μm fluxes are then

$$S^{\mathrm{pred}}_{10\,\mu\mathrm{m}} = 1.1\ \mathrm{Jy}\left(\frac{N_{uv}/N_{\mathrm{Br}\alpha}}{11.8}\right)\left(\frac{S_{\mathrm{Br}\alpha}}{10^{-12}\ \mathrm{ergs\ s^{-1}\ cm^{-2}}}\right).$$

This relation is independent of distance but is dependent on n_e and T_e through the ratio $N_{uv}/N_{\mathrm{Br}\alpha}$, and is quite dependent on grain properties. We expect that this is an upper limit and that a more reasonable value is probably a factor of 2–3 smaller, because the dust emissivity should flatten for wavelengths $\gtrsim 4$ μm. The grain temperature is probably not appreciably smaller than 200 K if these regions are similar to Galactic H II regions (e.g., Thronson, Campbell, and Harvey 1978; Lebofsky *et al.* 1978).

IV. OB STELLAR LUMINOSITY

The total luminosity of a population of OB stars with well-defined mass limits can be estimated from the ionizing flux. For star clusters with a Miller and Scalo initial mass function, the percentage of the total luminosity emitted at ionizing wavelengths, P_c, can be calculated as a function of the upper and lower mass limits (Ho and Haschick 1981). If the lower mass limit is less than 8 $M_\odot$, P_c depends only on the upper mass limit. For an upper mass limit of 30 $M_\odot$, $P_c \sim 0.1$. The total cluster luminosity is then

$$L_T \sim 10 L_{\lambda < \lambda_{\mathrm{Lyc}}} = 6.2 \times 10^{-44}\, L_\odot\, N_{uv}\ ,$$

TABLE 7

EXPECTED RATIO OF 10 μm TO TOTAL LUMINOSITY

	T_G					
$\lambda^{-\beta}$	100 K	150 K	200 K	300 K	400 K	500 K
	(μm^{-1})					
λ^0	3.7(−4)	8.9(−3)	3.1(−2)	6.8(−2)	7.3(−2)	6.3(−2)
λ^{-1}	1.4(−3)	2.2(−2)	5.8(−2)	8.5(−2)	6.8(−2)	4.7(−2)
λ^{-2}	4.1(−3)	4.4(−2)	8.5(−2)	8.3(−2)	5.0(−2)	2.8(−2)

where we assume that the mean energy of Lyman continuum photons is 15 eV. N_{uv} can be derived from $S_{\mathrm{Br}\alpha}$,

$$N_{uv} = 2.9 \times 10^{51}\ \mathrm{s}^{-1}\left(\frac{N_{uv}/N_{\mathrm{Br}\alpha}}{11.8}\right)\left(\frac{D}{1\ \mathrm{Mpc}}\right)^2\left(\frac{S_{\mathrm{Br}\alpha}}{10^{-12}\ \mathrm{ergs\ s^{-1}\ cm^{-2}}}\right).$$

Hence, the total cluster luminosity for an upper mass cutoff of 30 $M_\odot$ is

$$L_{\mathrm{OB}}^{\mathrm{pred}} \sim 1.8 \times 10^8\ L_\odot\left(\frac{N_{uv}/N_{\mathrm{Br}\alpha}}{11.8}\right)\left(\frac{D}{1\ \mathrm{Mpc}}\right)^2\left(\frac{S_{\mathrm{Br}\alpha}}{10^{-12}\ \mathrm{ergs\ s^{-1}\ cm^{-2}}}\right).$$

If the upper mass limit is doubled, L_T will be lowered by a factor of ~ 3.

REFERENCES

Aaronson, M., Mould, J., and Huchra, J. 1980, *Ap. J.*, **237**, 655.
Beck, S. C., and Beckwith, S. V. 1984, *M.N.R.A.S.*, **207**, 671.
Beck, S. C., Beckwith, S., and Gatley, I. 1984, *Ap. J.*, **279**, 563.
Beck, S. C., Lacy, J. H., Baas, F., and Townes, C. H. 1978, *Ap. J.*, **226**, 545.
Beck, S. C., Lacy, J. H., and Geballe, T. R. 1979, *Ap. J.*, **231**, 28.
Beck, S. C., Turner, J. L., and Ho, P. T. P. 1986, *Ap. J.*, **309**, 70 (Paper I).
Becklin, E. E., and Wynn-Williams, C. T. 1987, in *Star Formation in Galaxies*, ed. C. Persson (Pasadena: JPL), p. 643.
Beckwith, S., Evans, N. J., II, Gatley, I., Gull, G., and Russell, R. W. 1983, *Ap. J.*, **264**, 152.
Brocklehurst, M. 1971, *M.N.R.A.S.*, **153**, 471.
Carlstrom, J. E. 1988, in *Galactic and Extragalactic Star Formation*, ed. R. E. Pudritz and M. Fich (Dordrecht: Reidel), p. 571.
Condon, J. J. 1980, *Ap. J.*, **242**, 894.
Condon, J. J., Condon, M. A., Gisler, G., and Puschell, J. J. 1982, *Ap. J.*, **252**, 102.
Depoy, D. L., Becklin, E. E., and Geballe, T. R. 1987, *Ap. J. (Letters)*, **316**, L63.
de Vaucouleurs, G. 1979, *A.J.*, **84**, 1280.
de Vaucouleurs, G., de Vaucouleurs, A., and Corwin, H. G., Jr. 1976, *Second Reference Catalogue of Bright Galaxies* (Austin: University of Texas Press).
Draine, B. T., and Lee, H. M. 1984, *Ap. J.*, **285**, 89.
Duffy, P. B., Erickson, E. F., Haas, M. R., and Houck, J. R. 1987, *Ap. J.*, **315**, 68.
Duric, N., Seaquist, E. R., Crane, P. C., Bignell, R. C., and Davis, L. E. 1983, *Ap. J. (Letters)*, **273**, L11.
Feldman, F. R., Weedman, D. W., Balzano, V. A., and Ramsey, L. W. 1982, *Ap. J.*, **256**, 427.
Fischer, J., Simon, M., Benson, J., and Solomon, P. M. 1983, *Ap. J. (Letters)*, **273**, L27.
Gehrz, R. D., Sramek, R. A., and Weedman, D. W. 1983, *Ap. J.*, **267**, 551.
Genzel, R., Becklin, E. E., Wynn-Williams, C. G., Moran, J. M., Reid, M. J., Jaffe, D. T., and Downes, D. 1982, *Ap. J.*, **255**, 527.
Giles, K. 1977, *M.N.R.A.S.*, **180**, 578.
Hargrave, P. J. 1974, *M.N.R.A.S.*, **168**, 491.
Ho, P. T. P., and Haschick, A. D. 1981, *Ap. J.*, **248**, 622.
Ho, P. T. P., Turner, J. L., and Beck, S. C. 1989, in preparation.
Ho, P. T. P., Turner, J. L., Fazio, G. G., and Willner, S. P. 1989, *Ap. J.*, **344**, 135.
Hummel, E., van der Hulst, J. M., and Dickey, J. M. 1984, *Astr. Ap.*, **134**, 207.
Hummer, D. G., and Storey, P. J. 1987, *M.N.R.A.S.*, **224**, 801.
Kawara, K., Nishida, M., and Phillips, M. M. 1987, *Ap. J.*, **337**, 230.
Kellermann, K. I., and Pauliny-Toth, I. I. K. 1971, *Ap. Letters*, **8**, 153.
Kennicutt, R. C., Jr. 1979, *Ap. J.*, **228**, 704.
Lacy, J. H. 1980, in *IAU Symposium 96, Infrared Astronomy*, ed. C. G. Wynn-Williams and D. P. Cruikshank (Dordrecht: Reidel), p. 1.
Lebofsky, M. J., and Rieke, G. H. 1979, *Ap. J.*, **229**, 111.
Lebofsky, M. J., Sargent, D. G., Kleinmann, S. G., and Rieke, G. H. 1978, *Ap. J.*, **219**, 487.
Léger, A., and Puget, J. L. 1984, *Astr. Ap.*, **137**, L5.
Lester, D. F., Harvey, P. M., and Carr, J. 1988, *Ap. J.*, **329**, 641.
Lonsdale, C. J., Persson, S. E., and Matthews, K. 1984, *Ap. J.*, **287**, 95.
Love, R. 1972, *Nature*, **235**, 53.
Mezger, P. G., and Henderson, A. P. 1967, *Ap. J.*, **147**, 471.
Mirabel, I. 1982, *Ap. J.*, **260**, 75.
Neugebauer, G., *et al.* 1984, *Ap. J. (Letters)*, **278**, L1.
Phillips, M. M., Aitken, D. T., and Roche, P. F. 1984, *M.N.R.A.S.*, **207**, 25.
Rieke, G. H. 1976, *Ap. J. (Letters)*, **206**, L15.
Rieke, G. H., Cutri, R. M., Black, J. H., Kailey, W. F., McAlary, C. W., Lebofsky, M. J., and Elston, R. 1985, *Ap. J.*, **290**, 116.
Rieke, G. H., and Lebofsky, M. J. 1978, *Ap. J. (Letters)*, **220**, L37.
———. 1979, *Ann. Rev. Astr. Ap.*, **17**, 477.
Rieke, G. H., Lebofsky, M. J., Thompson, R. I., Low, F. J., and Tokunaga, A. T. 1980, *Ap. J.*, **238**, 24.
Rieke, G. H., Lebofsky, M. J., and Walker, C. E. 1988, *Ap. J.*, **325**, 679.
Rieke, G. H., and Low, F. J. 1972, *Ap. J. (Letters)*, **176**, L95.
Roche, P. F., and Aitken, D. K. 1985, *M.N.R.A.S.*, **213**, 789.
Sandage, A. 1984, *A.J.*, **89**, 621.
Sellgren, K. 1984, *Ap. J.*, **277**, 623.
Simon, M., Simon, T., and Joyce, R. R. 1979, *Ap. J.*, **227**, 64.
Soifer, B. T., Houck, J. R., and Neugebauer, G. 1987, *Ann. Rev. Astr. Ap.*, **25**, 187.
Spinrad, H., Bahcall, J., Becklin, E. E., Gunn, J. E., Kristian, J., Neugebauer, G., Sargent, W. L. W., and Smith, H. 1973, *Ap. J.*, **180**, 351.
Telesco, C. M. 1988, *Ann. Rev. Astr. Ap.*, **26**, 343.
Telesco, C. M., and Gatley, I. 1981, *Ap. J. (Letters)*, **247**, L11.
———. 1984, *Ap. J.*, **284**, 557.
Thompson, R. I. 1987, *Ap. J.*, **321**, 153.
Thronson, H. M., Campbell, M. F., and Harvey, P. M. 1978, *A.J.*, **83**, 1581.
Turner, J. L., Ho, P. T. P., and Beck, S. C. 1987, *Ap. J.*, **313**, 644 (Paper II).
Weedman, D. W., Feldman, F. R., Balzano, V. A., Ramsey, L. W., Sramek, R. A., and Wu, C. C. 1981, *Ap. J.*, **248**, 105.
Willner, S. P., Soifer, B. T., Russell, R. W., Joyce, R. R., and Gillett, F. C. 1977, *Ap. J. (Letters)*, **217**, L121.
Wynn-Williams, C. G., and Becklin, E. E. 1986, *Ap. J.*, **308**, 620.

SARA C. BECK: Department of Physics and Astronomy, Tel Aviv University, Ramat Aviv, Tel Aviv 69978, Israel

PAUL T. P. HO: Harvard-Smithsonian Center for Astrophysics, 60 Garden Street, Mail Stop 42, Cambridge, MA 02138

JEAN L. TURNER: Department of Astronomy, UCLA, 405 Hilgard Avenue, Los Angeles, CA 90024